J Math Chem (2010) 48:98–108
DOI 10.1007/s10910-009-9636-z

ORIGINAL PAPER

Numerical solution of nonlinear singularly perturbed problems by using a non-standard algorithm on variable stepsize implementation (CMMSE–2009)

Higinio Ramos · R. García-Rubio

Received: 23 October 2009 / Accepted: 23 November 2009 / Published online: 5 December 2009

Abstract In this article, we solve numerically singularly perturbed non-linear autonomous initial-value problems (IVPs) by using a non-standard algorithm on a variable stepsize implementation. On a recent article (Ramos et al. in J Math Chem, To appear) we had used nonuniform meshes for resolving the difficulties arising from the steep gradient of the solution in the initial layer. The present method is intended for solving the nonlinear problem using a nonuniform mesh originated by a suitable strategy provided for changing the stepsize. Numerical experiments are carried out to verify the efficiency and accuracy of the method, showing that the new procedure leads to better results than in (Ramos et al. in J Math Chem, To appear).

Keywords Singularly perturbed initial-value problems · Non-standard algorithm · Nonuniform meshes · Variable stepsize implementation

1 Introduction

Singular perturbation problems (SPPs) arise in various branches of applied areas like fluid dynamics, optimal control, chemical reactor theory, etc. Because of the presence of a small parameter multiplying the highest derivative, classical numerical methods fail to yield satisfactory results. Therefore, one has to seek some special methods for

H. Ramos (✉)
Scientific Computing Group, Universidad de Salamanca, Salamanca, Spain
e-mail: higra@usal.es

R. García-Rubio
Department of Applied Mathematics, Universidad de Salamanca, Salamanca, Spain
e-mail: rgr@usal.es

the numerical solution of SPPs. More details can be found in the books by Doolan et al. [6] and Miller et al. [14].

Experimental and theoretical results show that an adiabatic tubular reactor, in which there is occurring a simple first-order irreversible exothermic chemical reaction, can exhibit multiple stable steady states. The chemical and mathematical models of these processes can be found in the articles of Aris [1], and Burghardt and Zaleski [3]. The mathematical models of these chemical reactions are differential equations with the highest order derivative multiplied by a small positive parameter.

First-order differential equations are frequently employed for describing the dynamics of chemical reactions [2,5,11,12,19]. In this article, we present a procedure for numerically solving the nonlinear autonomous IVP

$$\begin{cases} \varepsilon\, u'(x) = f(u), \quad x \in \overline{D} = [0,1] \\ u(0) = A, \end{cases} \tag{1}$$

where $0 < \varepsilon \ll 1$ is a small parameter (the viscosity coefficient) and $u,\ f(u) \in \mathbb{R}$. We assume that the IVP in (1) admits a unique solution having an initial layer at $x = 0$. In [6], they have solved the nonlinear IVP (1) by exponentially fitted difference (EFD) schemes after linearizing it by Newton's quasilinearization.

O'Malley [15] has studied the asymptotic behavior of the solution of the IVPs. Numerical schemes for linear IVPs are studied in the book by Doolan et. al. [6] by using EFD schemes. Miller derived an optimal uniform difference scheme for singularly perturbed linear IVPs in [13]. Farrell [7] proposed a class of uniformly convergent optimal schemes for linear stiff initial-value problems. To apply these methods to nonlinear problems of the type (1), one has to linearize the problem. Alternately, one can use classical finite difference schemes to linear SPPs on some layer resolving meshes. One can get more insight about the application of Shishkin mesh to linear IVPs in the book [14]. In [16] a non-standard explicit algorithm was used for solving a particular SPP, although the application for a wide range of such kind of problems has not been studied.

Here, in this article, we directly solve the nonlinear IVP (1) by the non-standard algorithm in [18] using the nonuniform mesh provided by using a strategy for changing the stepsize. In [17] the non-standard algorithm has been applied on selected nonuniform meshes, showing that the use of nonuniform meshes is essential for numerically solving singularly perturbed IVPs of the form in (1). Now, the nonuniform mesh is not chosen in advanced, but is generated along the integration procedure based on a suitable strategy for changing the stepsize.

The paper is organized as follows: Section 2 reproduces the non-standard algorithm in [17] for the IVP (1). The formulation of the local truncation error in an appropriate way for applying the strategy for changing the stepsize is given in Sect. 3. In Sect. 4 we provide the strategy for selecting the stepsize value on each step. Numerical results are given in Sect. 5 for different examples compared with the results in [17]. Finally, some conclusions puts an end to the paper.

2 The non-standard algorithm (NSA)

Let the mesh points of $\overline{D} = [0, 1]$ be

$$x_0 = 0,\ x_i = \sum_{k=0}^{i-1} h_k,\ h_k = x_{k+1} - x_k,\ x_N = 1, \quad i = 1, 2, \ldots, N-1.$$

Suppose we have solved numerically the problem in (1) up to the mesh point x_n, and assuming the localization hypothesis $u_n = u(x_n)$, we want to obtain an approximate value, u_{n+1}, for the solution at the point $x_{n+1} = x_n + h_n$, that is, $u_{n+1} \simeq u(x_{n+1})$. For this purpose we consider on the interval $[x_n, x_{n+1}]$ the approximation of the IVP

$$\varepsilon\, u' = f(u), \qquad u(x_n) = u_n, \tag{2}$$

by the IVP given by

$$\varepsilon\, z' = f_n + J_n\,(z - u_n) + \frac{1}{2}\, H_n\,(z - u_n)^2\,, \qquad z(x_n) = u_n\,, \tag{3}$$

where

$$f_n = f(u_n)\,, \qquad J_n = \frac{\partial\, f(u)}{\partial\, u}(u_n)\,, \qquad H_n = \frac{\partial^2\, f(u)}{\partial\, u^2}(u_n)\,, \tag{4}$$

that is, we have approximated on $[x_n, x_{n+1}]$ the function $f(u)$ by its second-order Taylor polynomial constructed at the point $u = u_n$. We can solve the problem in (3) exactly, that is to say, without local truncation error, by using the difference scheme

$$z_{n+1} = \begin{cases} z_n - \dfrac{2\,\tan\left(\frac{d\,h_n}{2\,\varepsilon}\right)}{-d + (b + 2\,c\,u_n)\,\tan\left(\frac{d\,h_n}{2\,\varepsilon}\right)}\, f_n\,, & \Delta_n > 0\,, \\ z_n - \dfrac{2\,\tanh\left(\frac{d\,h_n}{2\,\varepsilon}\right)}{-d + (b + 2\,c\,u_n)\,\tanh\left(\frac{d\,h_n}{2\,\varepsilon}\right)}\, f_n\,, & \Delta_n < 0\,, \\ z_n - \dfrac{2\,h_n}{-2\,\varepsilon + h_n\,(b + 2\,c\,u_n)}\, f_n\,, & \Delta_n = 0\,, \end{cases} \tag{5}$$

where

$$\begin{aligned} a &= f_n - u_n\, J_n + \frac{1}{2}\, H_n\, u_n^2 \\ b &= J_n - u_n\, H_n \\ c &= \frac{1}{2}\, H_n \\ \Delta_n &= -b^2 + 4\,a\,c \\ d &= \sqrt{|\Delta_n|}\,. \end{aligned}$$

After applying this scheme we will take as approximation for the true solution of (1) at x_{n+1} the value $u_{n+1} = z_{n+1}$. Repeating the procedure along the nodes on the integration interval a discrete solution for the problem in (1) will be obtained.

3 Expressions for the local truncation error

We assume that the solution $u(x)$ of (1) is sufficiently smooth. By using Taylor series expansion one can obtain the following local truncation error (see [17,18])

$$T_{n+1} = \begin{cases} \frac{1}{12}\,\rho_0(u(x_n))\,h_n^3 + \mathcal{O}(h_n^4)\,, & \Delta_n = 0\,, \\ \frac{1}{24}\,\rho_1(u(x_n))\,h_n^4 + \mathcal{O}(h_n^5)\,, & \Delta_n \neq 0\,, \end{cases}$$

where the terms $\rho_0(u(x))$, $\rho_1(u(x)))$ have the form

$$\rho_0(u(x)) = \frac{-3\,u''(x)^2 + 2\,u'(x)\,u^{(3)}(x)}{u'(x)}\,,$$
$$\rho_1(u(x)) = \frac{3\,u''(x)^3 - 4\,u'(x)\,u''(x)\,u^{(3)}(x) + u'(x)^2\,u^{(4)}(x)}{u'(x)^2}\,.$$

Alternatively, in view of the differential equation in (1) the local truncation error may be expressed in the equivalent form

$$T_{n+1} = \begin{cases} \frac{1}{12\,\varepsilon^3}\,f_n\left(2\,f_n\,H_n - J_n^2\right)\,h_n^3 + \mathcal{O}(h_n^4)\,, & \Delta_n = 0\,, \\ \frac{1}{24\,\varepsilon^4}\,f_n^3\,K_n\,h_n^4 + \mathcal{O}(h_n^5)\,, & \Delta_n \neq 0\,, \end{cases} \tag{6}$$

where f_n, J_n, H_n are as in (4), and

$$K_n = \frac{\partial^3 f(u)}{\partial\, u^3}(u_n)\,.$$

Note that, with the exception of K_n, all the terms in the principal term of the local truncation error in (6) are calculated through the application of the method on each step, and so this form is more appropriate in order to apply the strategy in the next section.

4 Strategy for changing the stepsize

In [17] some nonuniform meshes were presented for solving the problem in (1). In the initial layer region, one requires a fine grid to obtain better approximation for the numerical solution, while a coarse mesh is enough in the outer region, where the solution behaves smoothly.

The best results for the numerical examples in [17] were obtained using a proper combination of Shishkin and Jain meshes [9]. More precisely, first we divided the

domain [0, 1] into two subdomains as $\overline{D} = [0, \tau) \cup [\tau, 1]$ and placed $N/2$ points uniformly in the subdomain $[0, \tau)$, and $N/2$ points nonuniformly in $[\tau, 1]$ by following the idea of the nonuniform mesh as given in [17]. One can notice that in the Shishkin mesh there is a big deviation between the fine and coarse meshes at the transition point. By this way we could slowly switch over from fine mesh to coarse mesh at the transition point. Indeed, this idea worked very well for the test examples given in [17].

The method in [17] was formulated using a fixed stepsize h. The appearance of the h_n in (5) was merely to indicate that is a one-step method, and so we can change the stepsize accordingly with a suitable strategy. In [17] this strategy consisted in the election of a priori nonuniform mesh related with the peculiarities of the problem in (1). However, as some authors have remarked, to be efficient, an integrator based on a particular formula must be suitable for a variable stepsize formulation [8,10]. There are mainly two ways to do that, using a formula where the coefficients depend on the ratios of the step sizes (as in the variable-coefficient linear multistep codes) or using a second method (as in the embedding Runge-Kutta pairs). In all the cases the goal is to adjust the step sizes so as to keep the estimated local errors smaller than a given tolerance and, at the same time, solve the problem as efficiently as possible [24]. So, a reliable estimate of the local error is needed. For that purpose we will consider the principal term of the local truncation error in (6) which will be used as an estimate of the local error on each step, that is

$$ERR = \begin{cases} \frac{1}{12\,\varepsilon^3}\, f_n \left(2\, f_n\, H_n - J_n^2\right)\, h_n^3\,, & \Delta_n = 0\,, \\ \frac{1}{24\,\varepsilon^4}\, f_n^3\, K_n\, h_n^4\,, & \Delta_n \neq 0\,, \end{cases} \tag{7}$$

The strategy considered here for changing the step size is that used on multistep codes, [4,10,23]: given a tolerance, TOL, for a selected norm, $\|\cdot\|$, the classical stepsize prediction derived from equating this tolerance to the norm of the estimate of the local error yields a new stepsize h_{new} given by

$$h_{\text{new}} \approx \nu h_{\text{old}} \left(\frac{TOL}{\|ERR\|}\right)^{1/(p+1)} \tag{8}$$

where p is the order of the method, and ν is a safety factor whose purpose is to avoid failed steps and usually takes values on the interval [0, 1]. In view of (7) and taking $h_{\text{old}} = h_n$, the new stepsize for the method in the above sections will result in

$$h_{\text{new}} = h_{n+1} = \begin{cases} \nu\, \varepsilon \left(\frac{12\, TOL}{\|\, f_n (2\, f_n\, H_n - J_n^2)\|}\right)^{1/3}, & \Delta_n = 0\,, \\ \nu\, \varepsilon \left(\frac{24\, TOL}{\|\, f_n^3\, K_n\|}\right)^{1/4}, & \Delta_n \neq 0\,, \end{cases} \tag{9}$$

where due to the presence of the small factor ε we take $\nu = \nu(\varepsilon) = \varepsilon^{\alpha}\,, \alpha < 0$ in order to avoid a large number of steps.

Although there are different strategies for selecting the size of the initial step, h_{ini}, (see [23,26]), we can take a very small value as in [22], and then the algorithm will correct this value if necessary in accordance with the changing stepsize strategy.

5 Numerical results

To verify the accuracy and efficiency of the present method, we have applied it to various test problems. The numerical results are presented in terms of maximum pointwise errors in the tables. Our main goal is to show the better performance of the method in variable stepsize formulation on nonuniform layer-resolving meshes provided by the strategy for changing the stepsize based on an estimate of the local truncation error.

We present the same test examples as in [17], which will be used to compare the numerical results obtained by the NSA using the nonuniform mesh II in [17] (which showed the best performance) and the implementation in this article. The value of α in $\nu = \varepsilon^{\alpha}$ has been taken after numerical experiments as $\alpha = -3/4$. Although this is a variable stepsize method we have used a shooting-like procedure to determine the value of TOL for which the number of variable steps equals the number of steps on the nonuniform mesh in [17]. The time used in both cases was similar. The tables show the maximum absolute error along the integration interval with the method in this article compared with the corresponding errors with the nonuniform mesh in [17]. The initial step has been taken for all examples as $h_{\text{ini}} = 2 \times 10^{-10}$.

Example 1 The first example is the nonlinear IVP given by

$$\begin{cases} \varepsilon\, u' = \exp(-u), \quad x \in [0, 1] \\ u(0) = 0, \end{cases}$$

whose exact solution is

$$u(x) = \log\left(1 + \frac{x}{\varepsilon}\right).$$

For each ε the maximum of the absolute errors on the nodal points in the integration interval is obtained by

$$E_{\varepsilon}^{N} = \max_{x_j \in [0,1]} |u(x_j) - u_j|.$$

Table 1 corresponds to the data of the NSA on nonuniform mesh II compared with the variable stepsize formulation of the nonstandard method. One can see how the proposed scheme provides better results with an increase of one order of accuracy.

Figure 1 corresponds to Example 1, where the sequence of stepsizes on the variable stepsize formulation have been plotted for $\varepsilon = 10^{-5}$ and $N = 128$. We observe how the stepsizes are increasing as the integration proceeds going away from the origin. The final value for the stepsize has been chosen deliberately so that the last node is the endpoint of the interval of integration.

Table 1 Maximum absolute errors for Example 1 by NSA using different implementations

ε	Mesh points	Maximum absolute errors (E_ε^N)	
		Nonuniform mesh II	Variable stepsize
10^{-2}	16	1.8475×10^{-2}	1.8619×10^{-3}
10^{-3}	32	7.5501×10^{-3}	5.6657×10^{-4}
10^{-4}	64	1.8203×10^{-3}	1.4809×10^{-4}
10^{-5}	128	3.7546×10^{-4}	3.4420×10^{-5}
10^{-6}	256	7.2359×10^{-5}	6.9974×10^{-6}

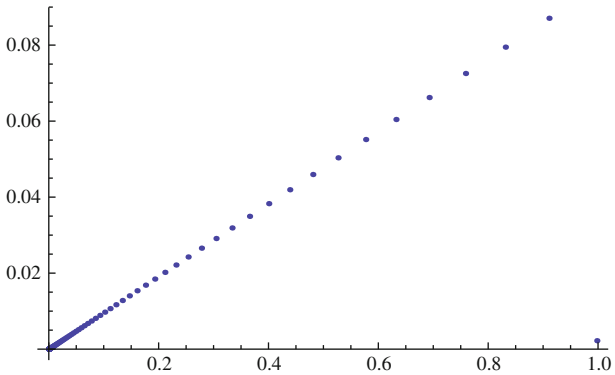

Fig. 1 Stepsizes used with NSA on variable stepsize implementation for Problem 1, $\varepsilon = 10^{-5}$, $N = 128$

Example 2 The following nonlinear IVP is a kinetic equation used to describe time evolution of adsorption under nonequilibrium conditions [12]

$$\begin{cases} \varepsilon\, u' = (1-u)^2, & x \in [0,1] \\ u(0) = 0.1 \end{cases}$$

The exact solution of the IVP is given by

$$u(x) = \frac{9\,x + \varepsilon}{9\,x + 10\,\varepsilon}\,.$$

The maximum absolute errors for this example are close to the machine precision for nonuniform mesh-II. This is because the non-standard scheme integrates this IVP without local truncation error, and the only error committed here is the round-off error. For the variable stepsize implementation we observe that in (7) it is $K_n = 0$ and so one can take just one step and the method will result to be exact (except for the round-off error).

Table 2 Maximum absolute error E_ε^N for Example 3 by NSA using different implementations

ε	Mesh points	Maximum absolute errors (E_ε^N)	
		Nonuniform mesh II	Variable stepsize
10^{-2}	16	1.3753×10^{-3}	7.2327×10^{-5}
10^{-3}	32	9.4651×10^{-5}	4.2756×10^{-6}
10^{-4}	64	1.5086×10^{-5}	3.4386×10^{-7}
10^{-5}	128	2.9757×10^{-6}	3.5179×10^{-8}
10^{-6}	256	5.5314×10^{-7}	3.8902×10^{-9}

Example 3 The next example is the IVP given by

$$\begin{cases} \varepsilon\, u' = \sin(u), & x \in [0, 1] \\ u(0) = u_0, \end{cases}$$

whose exact solution is

$$u(x) = 2\,\mathrm{arccot}\left(\exp\left(\frac{-x}{\varepsilon}\right)\cot\left(\frac{u_0}{2}\right)\right).$$

We take $u_0 \in (\pi/2, \pi)$ in order to assure the existence of a boundary layer at the initial point.

For this problem we have considered $u_0 = 2$ for the numerical tests. In this case it is $u'(x) > 0$ and the solution grows towards the fixed point $u(x) = \pi$.

For this problem, we have applied the non-standard algorithm on nonuniform mesh-II and the variable stepsize implementation. The maximum absolute errors obtained with both implementations are given in Table 2.

In Fig. 2 the plots of the absolute errors (up) and the sequence of stepsizes (down) for Example 3 on an interval containing the initial layer using the variable stepsize implementation are shown for $\varepsilon = 10^{-5}$, and $N = 128$.

Example 4 The following nonlinear IVP models the kinetic behavior of biosorption [11,21]:

$$\begin{cases} \varepsilon\, u' = u - u^3, & x \in [0, 1] \\ u(0) = 0.1\,. \end{cases}$$

The exact solution of this IVP is

$$u(x) = \frac{\exp\left(\frac{x}{\varepsilon}\right)}{\sqrt{99 + \exp\left(\frac{2x}{\varepsilon}\right)}}.$$

Table 3 corresponds to Example 4 for *NSA* on nonuniform mesh II and on variable stepsize implementation. The maximum pointwise errors of Table 3 reveal the better performance of the method on variable stepsize mode.

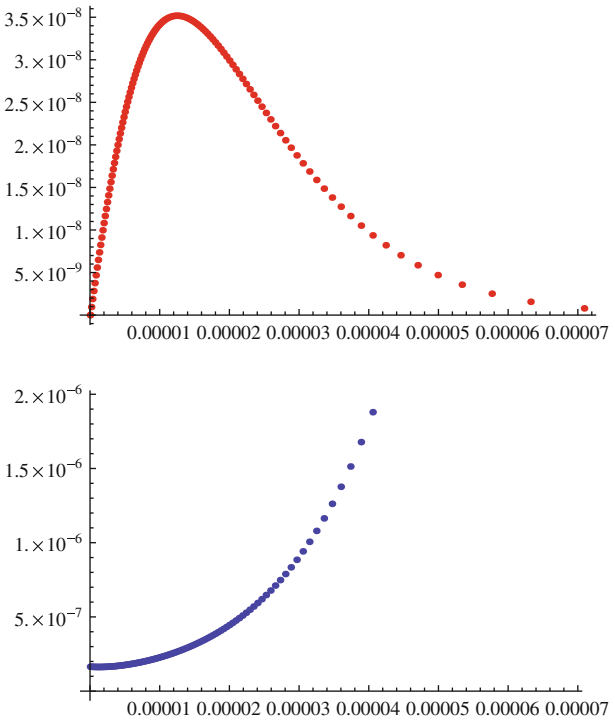

Fig. 2 Absolute errors (*up*) and sequence of stepsizes (*down*) for Problem 3 ($N = 128$, $\varepsilon = 10^{-5}$)

Table 3 Maximum absolute error E_ε^N for Example 4 by NSA using different implementations

ε	Mesh points	Maximum absolute errors	
		Nonuniform mesh II	Variable stepsize
10^{-2}	16	5.4840×10^{-4}	1.2145×10^{-3}
10^{-3}	32	8.2133×10^{-5}	5.9184×10^{-5}
10^{-4}	64	1.7949×10^{-5}	4.4481×10^{-6}
10^{-5}	128	3.5867×10^{-6}	4.2284×10^{-7}
10^{-6}	256	6.7191×10^{-7}	4.5367×10^{-8}

In Fig. 3, we plotted the absolute errors (up) and the sequence of stepsizes (down) obtained by the *NSA* using variable stepsizes for $\varepsilon = 10^{-5}$ and $N = 128$.

6 Conclusions

In this article, we have considered the implementation of the nonstandard method in [17] using a variable stepsize formulation. The method was intended for singularly perturbed nonlinear autonomous IVPs. The solution of these problems has a multiscale

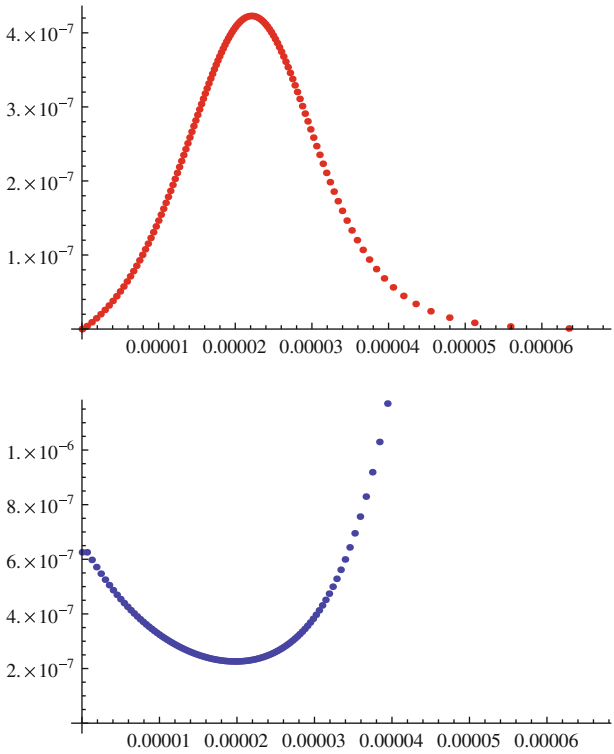

Fig. 3 Absolute errors (*up*) and sequence of stepsizes (*down*) for Problem 4 ($N = 128$, $\varepsilon = 10^{-5}$)

character, and in [17] it was shown the necessity of using special nonuniform meshes to solve these problems in order to capture the rapidly varying solution inside the initial layer. If one wants to apply the existing techniques in the literature, then the nonlinear IVP has to be linearized first and so one may loose many nice properties of the solution by linearizing the problem. In this paper we have shown that the nonuniform mesh resulting from the formulation in variable stepsize improves the performance of the method. The numerical results presented in the previous section reveal this fact.

Acknowledgments The authors wish to thank JCYL project SA050A08 and MICYT project MTM2008/05489 for financial support.

References

1. R. Aris, On stability criteria of chemical reaction engineering. Chem. Eng. Sci. **24**, 149–169 (1968)
2. W. Benzinger, A. Becker, K.J. Httinger, Chemistry and kinetics of chemical vapour deposition of pyrocarbon: I. Fundamentals of kinetics and chemical reaction engineering. Carbon **34**, 957–966 (1996)
3. A. Burghardt, T. Zaleski, Longitudinal dispersion at small and large Peclet numbers in chemical flow reactors. Chem. Eng. Sci. **23**, 575–591 (1968)
4. M. Calvo, J.I. Montijano, L. Randez, On the change of step size in multistep codes. Numer. Alg. **4**, 283–304 (1993)

5. M. Danish, R.K. Sharma, S. Ali, Gas absorption with first order chemical reaction in a laminar falling film over a reacting solid wall. Appl. Math. Model. **32**, 901–929 (2008)
6. E.P. Doolan, J.J.H. Miller, W.H.A. Schildres, *Uniform Numerical Methods for Problems with Initial and Boundary Layers* (Boole Press, Dublin, 1980)
7. P.A. Farrell, Uniform and optimal schemes for stiff initial-value problems. Comp. Math. Appl. **13**, 925–936 (1987)
8. E. Hairer, S.P. Norsett, G. Wanner, *Solving Ordinary Differential Equations I* (Springer, Berlin, 1987)
9. M.K. Jain, *Numerical Solution of Differential Equations* (Wiley Eastern Limited, New Delhi, 1984)
10. J.D. Lambert, *Numerical Methods for Ordinary Differential Systems* (Wiley, England, 1991)
11. Y. Liu, L. Shen, A general rate law equation for biosorption. Biochem. Eng. J. **38**, 390–394 (2008)
12. Y. Liu, New insights into pseudo-second-order kinetic equation for adsorption. Colloids Surf. A **320**, 275–278 (2008)
13. J.J.H. Miller, Optimal uniform difference schemes for linear initial-value problems. Comp. Math. Appl. **12**, 1209–1215 (1986)
14. J.J.H. Miller, E. O'Riordan, G.I. Shishkin, *Fitted Numerical Methods for Singular Perturbation Problems* (World Scientific, Singapore, 1996)
15. R.E. O'Malley, *Introduction to Singular Perturbation* (Academic Press, New York, 1974)
16. H. Ramos, A non-standard explicit integration scheme for initial-value problems. Appl. Math. Comput. **189**, 710–718 (2007)
17. H. Ramos, J. Vigo-Aguiar, S. Natesan, R. Garca-Rubio, M.A. Queiruga, Numerical solution of nonlinear singularly perturbed problems on nonuniform meshes by using a non-standard algorithm. J. Math. Chem. To appear. doi:10.1007/s10910-009-9625-2
18. H. Ramos, J. Vigo-Aguiar, A new algorithm appropriate for solving singular and singularly perturbed autonomous initial-value problems. Int. J. Comp. Math. **85**, 603–611 (2008)
19. C.V. Rao, D.M. Wolf, A.P. Arkin, Control, exploitation and tolerance of intracellular noise. Nature **420**, 231–237 (2002)
20. M.J.O. Reilly, E. O'Riordan, A Shishkin mesh for a singularly perturbed Riccati equation. J. Comput. Appl. Math. **182**, 372–387 (2005)
21. W. Rudzinski, W. Plazinski, Kinetics of solute adsorption at solid/solution interfaces: a theoretical development of the empirical pseudo-first and pseudo-second order kinetic rate equations, based on applying the statistical rate theory of interfacial transport. J. Phys. Chem. B **110**, 16514–16525 (2006)
22. A.E. Sedgwick, An effective variable order variable step Adams method. Dept. of Computer Science Rept. 53. (University of Toronto, Toronto, Canada, 1973)
23. L.F. Shampine, M.K. Gordon, *Computer Solution of Ordinary Differential Equations. The Initial Value Problem* (Freeman, San Francisco, CA, 1975)
24. L.F. Shampine, A. Witt, Control of local error stabilizes integrations. J. Comp. Appl. Math. **62**, 333–351 (1995)
25. J. Vigo-Aguiar, S. Natesan, A parallel boundary value technique for singularly perturbed two-point boundary value problems. J. Supercomp. **27**, 195–206 (2004)
26. H.A. Watts, Starting step size for an ODE solver. J. Comp. Appl. Math. **9**, 177–191 (1983)